Supporting Information

Pt-free solar driven photoelectrochemical hydrogen fuel generation using 1T MoS_2 co-catalyst assembled CdS QDs/TiO_2 photoelectrode

R. Raja,[a] P. Sudhagar,[b*] Anitha Devadoss,[b] C. Terashima,[b] L. K. Shrestha,[c] K. Nakata,[b] R. Jayavel,[a*] K. Ariga,[c] and A. Fujishima[b]

S1. Experimental:

All reagents were received from Sigma-Aldrich and used without further purification.

(a) Synthesis and fabrication of TiO_2 electrode:

The TiO_2 nanocrystalline powder was synthesized by hydrothermal process as follows: A mixture of 75 mL of ethanol and 5 mL of acetic acid was prepared. Then 10 mL of titanium isopropoxide (nacalai tesque, Japan) was slowly added to the above mixture. The solution was vigorously stirred for 2h and transferred into 100 mL of Telfon coated autoclave, sealed and maintained at 150 °C for 15h in the oven. After the reaction time, the resulting mixture was centrifuged 3 to 4 times with ethanol and finally dried in vacuum at 60 °C for 12 h.

The as-synthesized TiO_2 powder is mixed with ethyl cellulose (Sigma Aldrich) and alpha terpineol (Sigma Aldrich) binder. Further this mixture was grounded well in mortar for 20 min manually and transformed to three dimensional rotor milling for 30 minutes (2000 RPM). The resultant TiO_2 paste was coated on well-cleaned fluorinated tin-oxide (Solarnix) coated glass substrates by doctor blade technique (thickness is ~6 micron). Subsequently it was sintered at 450 °C for 2 hrs in air atmosphere.

(b) Facial synthesis of MoS_2:

The MoS_2 nanosheets were prepared by chemical exfoliation method according to Coleman *et al*.[1] with slight modification. For instance, equal weight of bulk MoS_2 powder (Sigma-Aldrich) was mixed with mL of N-vinyl pyrrolidinone (NVP) (1 mg/ mL) (Tokyo chemical industries, Japan). Further this slurry was ultrasonicated for 96 h and finally the fine dispersion was collected through centrifuge process (1500 RPM).

(c) CdS QDs-sensitization:

The CdS QDs were prepared by SILAR process as is reported by Sudhagar *et al*.[2] The different chemical baths were prepared with Cd^{2+} cationic and S^{2-} anionic precursors in 0.5 M cadmium acetate in ethanol and 0.5 M Na_2S in methanol, respectively. The resultant TiO_2 mesoporous electrode was dipped in each chemical bath for 15 minutes (one cycle). After each bath, the TiO_2 electrode was completely rinsed by immersing in the corresponding solvent to remove the chemical residuals from the surface and then dried in nitrogen.

(d) TiO_2-CdS-ZnS and TiO_2-CdS-MoS_2 electrodes:

For preparing photoanode 4 cycles of CdS coating was carried out on TiO_2 and subsequently the passivation layer of ZnS was coated after SILAR sensitization, by alternately dipping it into 0.1 M $Zn(CH3COO)_2$ and 0.1 M Na_2S solutions for 1 min per dip and subsequently rinsing with water. Two SILAR cycles were employed for ZnS coating.

In the case of counter electrode 2 cycles of CdS was coated on TiO_2 and subsequently the MoS_2 was coated by spin coating (2000 RPM) from exfoliated MoS_2 solution. Finally it was heated at 80 °C for 10 minutes.

(e) Characterization details:

The crystalline phases of the TiO_2 and TiO_2/CdS QDs films were studied by X-ray diffraction (XRD) using a diffractometer (Rigagu Denki Japan) with CuKα radiation. The morphology of CuO electrode was characterized using the field emission scanning electron microscope (JSM-7500F JEOL)). The HRTEM images were recorded using JEOL. The optical absorption and diffused reflectance spectra of the electrodes were recorded in the range of 350–900 nm using a V670 JASCO UV-Vis spectrophotometer. The photoluminescence spectra were recorded using Horiba-Jobin-Yvon T64000 with a excitation wavelength of 325 nm.

(f) Photoelectrochemical (PEC) cells measurements:

The photoelectrochemical measurements were carried out using PGSTAT 128N-Autolab potentiostat. The two electrode PEC cell was configured with as prepared photoanode (TiO_2-CdS (4 cycle)-ZnS) and TiO_2-CdS (2 cycle)-MoS_2 as explained in S1 (d). These two electrodes were attached back to back as is illustrated in scheme 1(c) from main manuscript. In order to compare the catalytic performance of TiO_2-CdS-MoS_2 electrode, the conventional Pt wire was

also tested as CE with same photoanode (TiO_2-CdS-ZnS). An aqueous solution containing 0.25 M Na_2S and 0.35 M Na_2SO_3 as sacrificial hole scavenger was used as the electrolyte to prevent photocorrosion of the QDs. The nitrogen gas was bubbled for 30min before testing to avoid the presence of oxygen (electron acceptor) in the solution. The pH of the electrolyte was 12.1. The electrodes were illuminated using a solar simulator (HAL-320, ASAHI Spectra, Japan), with 400 nm cut off filter. The light intensity (100 mW/cm^{-2}) was adjusted with a Si-photodiode.

The output gas from photoelectrochemical cell was collected at applied potential of 0 V and 1V vs RHE for 1 hr duration from the head space using an air-tight gas syringe through the manual sampling port in the top of the chamber (flexible cork made of Teflon) and further subjected to gas chromatographic analysis to evaluate the constituents of the gaseous products. For ensure the reproducibility, the different set up photoelectrodes was tested and average quantity of hydrogen gas is reported.

S2. Surface morphology of the photoelectrode: SEM analysis

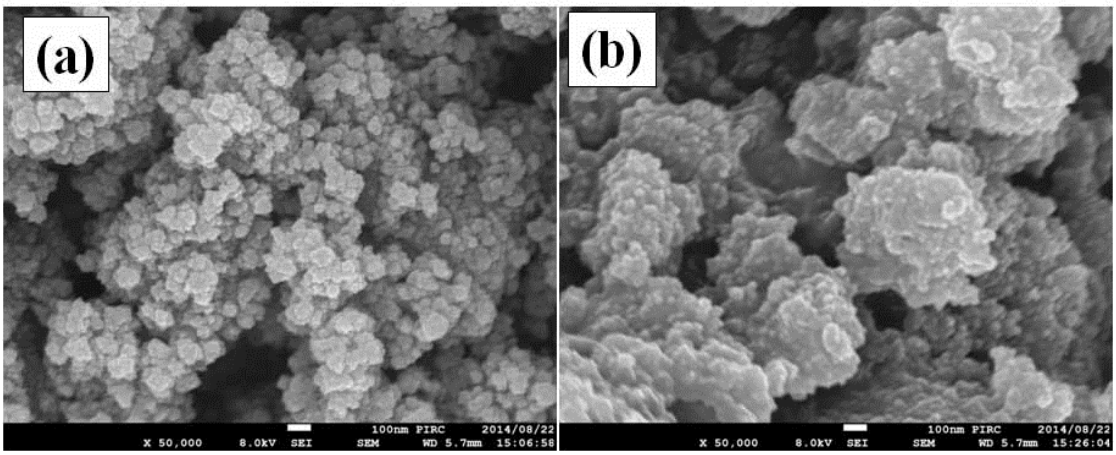

Figure S2. Surface morphology of (a) CdS QDs-coated TiO_2 mesoporous electrode without MoS_2 co-catayst and (b) MoS_2 coated CdS QDs/TiO_2 mesoporous electrode.

S3. Crystallite phases of MoS_2: TEM analysis

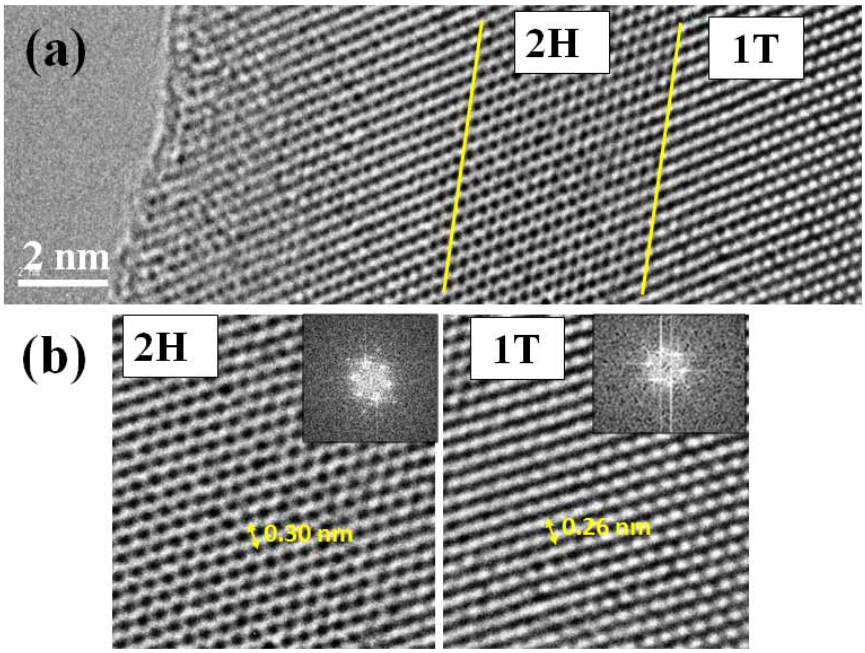

Figure S3. (a) HRTEM images of exfoliated MoS_2 (b) high magnification images of 1T and 2H phases.

S4. Crystallite analysis: XRD

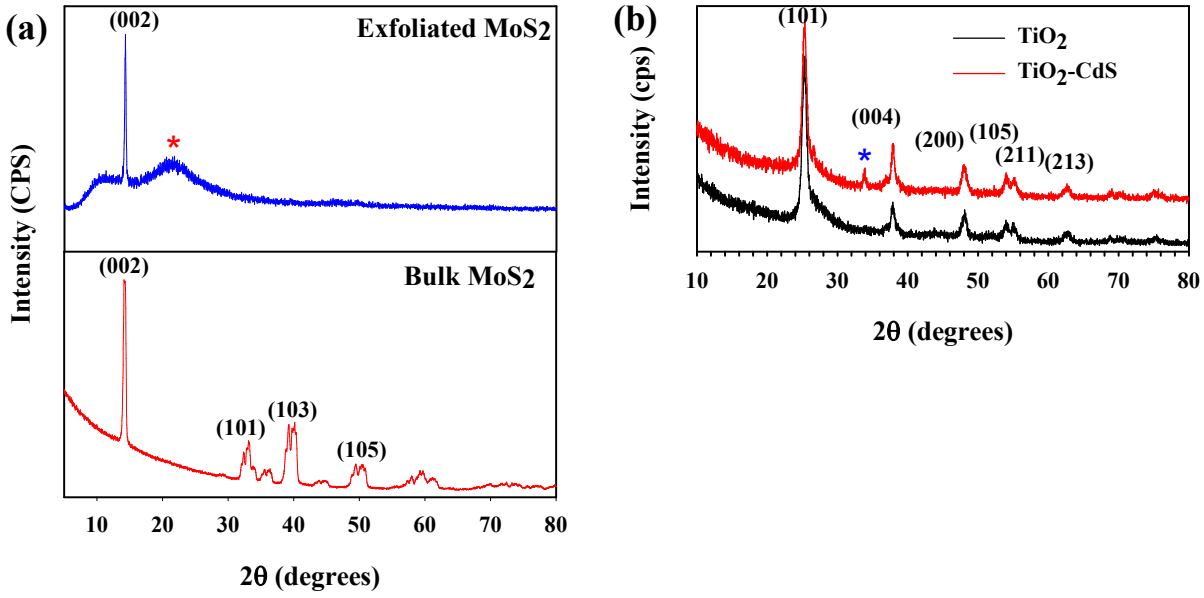

Figure S4. (a) XRD results of bulk MoS_2 powder and exfoliated MoS_2 coated on corning glass substrate; (b) XRD results of pristine and CdS QDs sensitized TiO_2 mesoporous electrode (the crystallite peak contributed from substrate is indicated with * symbol).

The crystallite structure of bulk and exfoliated MoS_2 is studied with by X-ray diffraction spectra using a diffractometer (Rigaku Denki Japan) with CuKα radiation. The d-spacing of the crystallite lattice and full-width half maximum of the peaks were analyzed by PDXL-2 software. From Fig. S4 (a), the crystallite peaks of bulk MoS_2 match with molybdenite structure (JCPDS 37-1492) exhibits with strong diffraction intensity at 2θ =14.1° corresponds to (002) crystallite phase and other small diffraction intensities at 2θ = 35.2°, 39.5° and 49.7° attributed to (101), (103) and (105) crystallite phases, respectively. In the case of exfoliated MoS_2 it exhibits strong diffraction intensity at 2θ =14.4° implies the predominant (002) crystallite phases suggesting the single layers in these sample.[3,4] The crystallite structure of TiO_2 electrode sintered at 450 °C, prepared from hydrothermal process is studied and presented in Fig. S4 (b), the predominant

diffraction peak was observed at ~ 2θ = 25.3° and 37.6° corresponds to (101) and (004) crystallite phases of anatase TiO_2 (JCPDS 21-1272). The peak corresponds to CdS (greenockite structure) at 26.4° may overlap with (101) TiO_2 peak is not able to detect separately.

S5. Optical property: exfoliated MoS_2

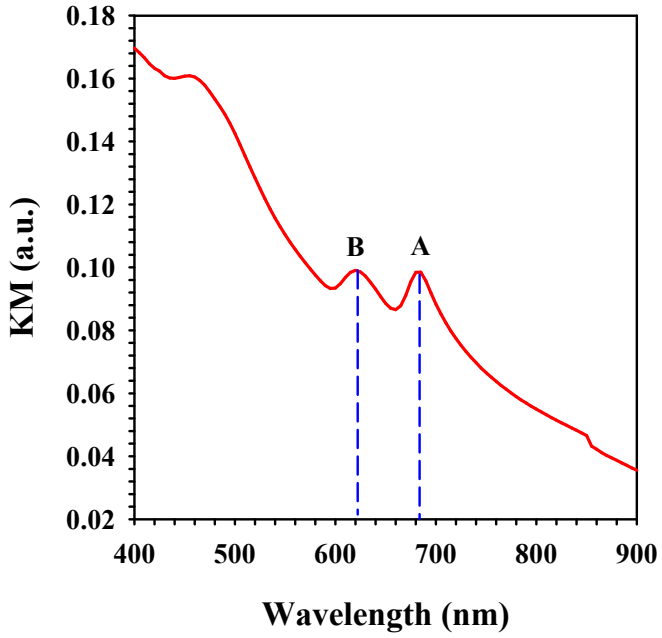

Figure S5. Optical absorbance spectra of chemically exfoliated MoS_2.

Fig. S5 shows the optical absorbance spectra of chemically exfoliated MoS_2 in N-Vinyl pyrrolidinone. It clearly depicts two prominent absorption peaks at ~682 nm (indicated as A) and ~620 (indicated as B) ensure the MoS_2.[5,6] The energy difference between excitons A and B originates from the spin-orbital splitting of the valence band.[7] The direct excitonic transitions at the K point of the first Brillouin zone produce the band gap in this system. The broad absorbance shoulder centered at ~ 450 nm attributed to the complicated C and D transitions.[7,8]

S6. Optical absorbance of front and back side electrodes:

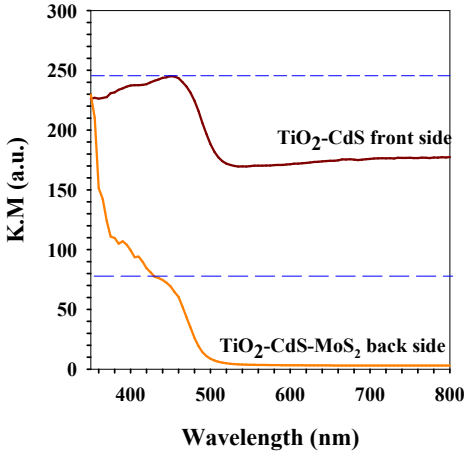

Figure S6. Optical absorbance of front side TiO_2/CdS/ZnS electrode and back side TiO_2/CdS/MoS_2 electrodes. Note that the optical absorbance of front side TiO2/CdS/ZnS electrode is corrected with FTO substrate and back side coating of TiO_2/CdS/MoS_2 is corrected by TiO2/CdS/ZnS electrode.

The utilization of single light source for illuminating both photoanode and cathode as is illustrated in scheme 1c in the main manuscript limits the illumination of back side electrode. For evaluating the quantity of light absorbed by front and back side electrodes, the fraction of light absorbance is evaluated individually. Fig. S6, shows the optical absorbance (Kulbelka Munk) of single (TiO2/CdS/ZnS) and double side assembled electrodes (TiO2/CdS/ZnS –front and TiO-2/CdS/MoS2-back) as is shown in scheme 1c. The FTO coated glass substrate and TiO2/CdS/ZnS electrode were used as reference electrodes for correcting the optical absorbance measurements of single and double side assembled electrodes, respectively. We found that the back side electrode absorbs three times lower than that of front side electrode due to the less light illumination avail after TiO2/CdS (4)/ ZnS front electrode as well due to the low coating cycles of CdS on back side electrode. However the high absorbance coefficient of CdS QDs manages the light absorbance quantity.

S7. Mott-Schottky plots

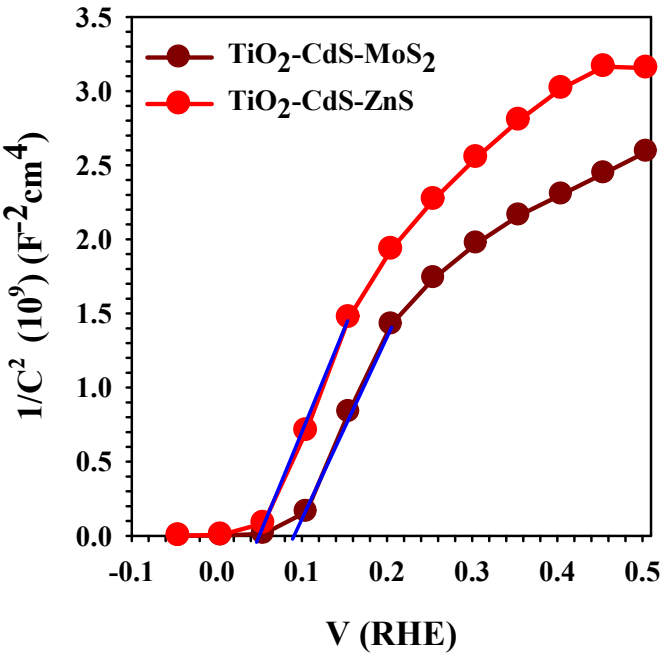

Figure S7. Mott–Schottky plots for TiO_2-CdS electrodes with and without MoS_2 coating.

The influence of MoS_2 coating on conducting band edge position of TiO_2/CdS was studied by using Mott–Schottky (MS) plots. The MS plots were obtained by impedance spectroscopy and the results are presented in Fig. S6 and the extrapolation of the Mott–Schottky plots ($1/C^2$ vs. V, electrode potential) was extracted using the following equation and the flat-band potential can be estimated.[9,10]

$$\frac{1}{C^2} = \frac{2}{N_D \varepsilon_0 \varepsilon_{TiO2} e}\left(E - E_{fb} - \frac{K_B T}{e}\right)$$

where C is the space charge capacitance, E the externally applied potential, E_{fb} the flatband potential at the semiconductor/electrolyte junction, N_D the donor density, ε_0 the permittivity of the free space, ε_{TiO2} the permittivity of the semiconductor electrode, e the elementary charge, k_BBoltzmann's constant, and T the operating temperature. The interception of x axis from $1/C^2$ vs. V plots provide the flat band potential of the materials. From Fig.S8, it is found to the V_{fb} =0.05 ±0.03 V vs RHE for TiO_2/CdS electrode and shifted to positive potential direction V_{fb} =0.09 ±0.03 V vs RHE by MoS_2 coating. This implies that the conduction band edge of MoS_2

is lower than CdS, which facilitates the photoelectron flow from CdS to MoS_2 for catalytic reaction.

S8. Electrochemical stability: hydrogen fuel generation

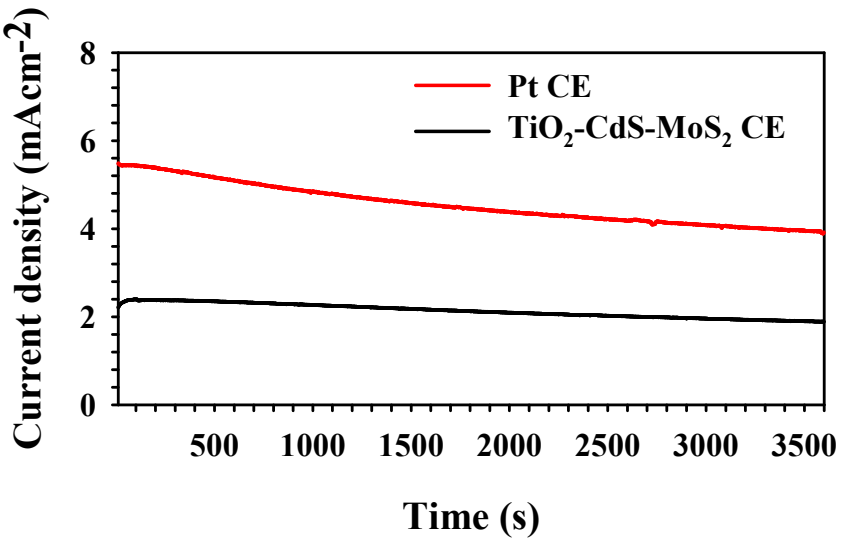

Figure S7. Chronoamperometry *J-V* plots of TiO_2/CdS/ZnS photoanode with different counter electrodes (measured at applied potential 1 V). The visible light illumination of 100 $mWcm^{-2}$ is applied for experiments (with 400 nm filter).

Reference:

1) J. N. Coleman, M. Lotya, A. O'Neill, S. D. Bergin, P. J. King, U. Khan, K. Young, A. Gaucher, S. De, R. J. Smith, I. V. Shvets, S. K. Arora, G. Stanton, H.-Y. Kim, K. Lee, G. T. Kim, G. S. Duesberg, T. Hallam, J. J. Boland, J. J. Wang, J. F. Donegan, J. C. Grunlan, G. Moriarty, A. Shmeliov, R. J. Nicholls, J. M. Perkins, E. M. Grieveson, K. Theuwissen, D. W. McComb, P. D. Nellist and V. Nicolosi, Science, 2011, **331**, 568.
2) P. Sudhagar, V. Gonzalez-Pedro, I. Mora-Sero, F. Fabregat-Santiago, J. Bisquert and Y. S. Kang, Journal of Materials Chemistry, 2012, **22**, 14228.
3) V. Stengl and J. Henych, Nanoscale, 2013, 5, 3387.
4) X. Shao, J. Tian, Q. Xue and C. Ma, Journal of Materials Chemistry, 2003, 13, 631.
5) K. F. Mak, C. Lee, J. Hone, J. Shan and T. F. Heinz, *Physical Review Letters*, 2010, **105**, 136805
6) G. Eda, H. Yamaguchi, D. Voiry, T. Fujita, M. Chen and M. Chhowalla, *Nano Letters*, 2011, **11**, 5111.
7) L. A. King, W. Zhao, M. Chhowalla, D. J. Riley and G. Eda, *Journal of Materials Chemistry A*, 2013, **1**, 8935.
8) L. Tao, H. Long, B. Zhou, S. F. Yu, S. P. Lau, Y. Chai, K. H. Fung, Y. H. Tsang, J. Yao and D. Xu, *Nanoscale*, 2014, **6**, 9713.
9) F. Fabregat-Santiago, G. Garcia-Belmonte, J. Bisquert, P. Bogdanoff and A. Zaban, Journal of The Electrochemical Society, 2003, **150**, E293.

10) J. Choi, P. Sudhagar, P. Lakshmipathiraj, J. W. Lee, A. Devadoss, S. Lee, T. Song, S. Hong, S. Eito, C. Terashima, T. H. Han, J. K. Kang, A. Fujishima, Y. S. Kang and U. Paik, RSC Advances, 2014, **4**, 11750.